

# Prediction of large linear-in- $k$ spin splitting for holes in the 2D GaAs/AlAs system

Jun-Wei Luo,<sup>1</sup> Athanasios N. Chantis,<sup>2</sup> Mark van Schilfgaarde,<sup>3</sup> Gabriel Bester,<sup>4</sup> and Alex Zunger<sup>1</sup>

<sup>1</sup>*National Renewable Energy Laboratory, Golden, Colorado 80401, USA*

<sup>2</sup>*Los Alamos National Laboratory, Los Alamos, New Mexico 87545, USA*

<sup>3</sup>*Arizona State University, Tempe, Arizona 85287, USA*

<sup>4</sup>*Max Planck Institute for Solid State Research, D-70569 Stuttgart, Germany*

(Dated: November 5, 2018)

## Abstract

The spin-orbit interaction generally leads to spin splitting (SS) of electron and hole energy states in solids, a splitting that is characterized by a scaling with the wavevector  $\mathbf{k}$ . Whereas for 3D bulk zincblende solids the electron (heavy hole) SS exhibits a cubic (linear) scaling with  $k$ , in 2D quantum-wells the electron (heavy hole) SS is currently believed to have a mostly linear (cubic) scaling. Such expectations are based on using a small 3D envelope function basis set to describe 2D physics. By treating instead the 2D system explicitly in a multi-band many-body approach we discover a large linear scaling of hole states in 2D. This scaling emerges from hole bands coupling that would be unsuspected by the standard model that judges coupling by energy proximity. This discovery of a linear Dresselhaus  $k$ -scaling for holes in 2D implies a different understanding of hole-physics in low-dimensions.

PACS numbers: 71.70.Ej, 73.21.Fg, 71.15.-m

Spin-orbit interaction causes the energy levels of 3D bulk-solids [1] and 2D quantum wells (QW's) [2] to exhibit a zero-field SS for sufficiently low-symmetry states. On the experimental side, attention has recently focused on spin of *holes* in 2D quantum-wells because of their spin Hall-effect [3] and in 0D quantum dots because of the highly coherent hole spin [4] and unusually long hole spin lifetime [5, 6], promising potential interesting applications in spintronic devices and solid state quantum computers. On the theoretical side, the long-standing tradition [1, 2, 7] has been to describe hole or electron spin physics in low-dimensional ( $< 3D$ ) nanostructures by an expansion in a rather small basis of 3D bulk envelope functions, using effective-mass approaches. In general, when the basis set is restricted, the resolution of the expansion is limited. Such low-resolution expansions can be “far sighted” [8] in that the actual atomistic symmetry of the nano object [9] is replaced by a fictitious higher symmetry, thus missing important degeneracy-splitting and inter-band coupling effects. The farsightedness can be cured by systematically increasing the basis set [10] or by introducing *ad-hoc* terms in the Hamiltonian intended to lower the symmetry [11, 12]. Both modifications come at the expense of introducing more parameters that are not calculable by the envelope function theory itself. Indeed, in the standard model for SS of nanostructures [13, 14, 15], one uses a phenomenological Hamiltonian where one needs to decide at the outset, which 3D bands couple in 2D by the spin-orbit interaction (SOI), rather than have the theory force such realization upon us. The potential of missing important physical interactions not selected to be present in the model Hamiltonian can be substantial [8].

The current state of the art for the hole states in 2D is illustrated by the work of Bulaev and Loss [13]. Starting from a bulk 3D Hamiltonian restricted to heavy-hole (HH) and light-hole (LH) bands (“ $4 \times 4$ ”), they have derived an effective  $2 \times 2$  Hamiltonian for the 2D heavy hole (hh0) subband, demonstrating an exact cancellation of the linear-in-k (Dresselhaus) terms [13]. This result (implying a pure, uncoupled hh0 state in low-dimensions) has been used in numerous theories of hole spin in 2D quantum-well and 0D quantum-dot systems, including in estimation of hole spin relaxation time [5], demonstration of intrinsic hole spin Hall Effect [16], and other hole spin related phenomena [17, 18, 19, 20]. We adopt instead a different approach in which the 2D nanostructures is viewed as a system in its own right, rather than express it in terms of a pre-selected basis drawn from a 3D system. We do so by solving the 2D band structure using explicitly the microscopic potential of the 2D system

under consideration, thus freeing us from the need to judge at the outset which selected 3D bands (e.g.,  $4 \times 4$  in Ref. 13) will couple in 2D. The results show that the linear term for *holes* is of the same order of magnitude as the well known linear term for *electrons* [15, 21]. This discovery of a linear Dresselhaus k-scaling for holes in 2D implies a different understanding of hole-physics in low-dimensions.

The central point of the approach utilized here is that the 3D and 2D systems are *each* described by their own microscopic Hamiltonian which is solved in basis sets whose sole property is that it produces a converged solution to the system at hand. Thus, the solution reflects only the underlying microscopic Hamiltonian, unmasked by issues of choices of bases or pre-selected Hamiltonian terms. We use a rather general microscopic Hamiltonian in the “*GW* representation”

$$H_{GW} = -\frac{1}{2}\nabla^2 + H_{so} + [V_{ext} + V_H + \Sigma], \quad (1)$$

where  $V_{ext}$  is the electron-ion potential,  $V_H$  is the interelectronic Hartree potential of the specific (3D or 2D) system;  $\Sigma = iG^0W$  is the self-energy with  $W$  being the screened Coulomb interaction and  $G^0 = 1/(\omega - H^0 \pm i\epsilon)$  is the Green’s function of a noninteracting Hamiltonian  $H^0$ . The physics represented in Eq. (1) includes the atomistic symmetry of the specific (2D or 3D) system specified by atomic position vectors in  $V_{ext}(\mathbf{R}_n - \mathbf{d}_{\alpha,j})$  and incorporates self-consistent electrostatic and exchange-and-correlation effects. This quasi-particle self-consistent *GW* (QSGW) scheme has been established as capable of predicting accurate bulk energy bands [22], including the Dresselhaus splitting in bulk GaAs [23, 24].

The approach described above is computationally intensive and can be readily applied only to rather small nanostructures. Thus, for computational expediency, when considering larger period quantum wells [e.g,  $(\text{GaAs})_n/(\text{AlAs})_n$  with  $n \gg 2$ ] we will map both the small- $n$  behavior and the  $n = \infty$  (bulk) QSGW solutions of Eq. (1) to a screened pseudopotential Hamiltonian that captures the former limits yet can be readily applied to orders of magnitude larger systems ( $10^6$  atoms were demonstrated in Ref. 8):

$$H_{PP} = -\frac{1}{2}\nabla^2 + H_{so} + \sum_{n,\alpha,j} v_\alpha(\mathbf{r} - \mathbf{R}_n - \mathbf{d}_{\alpha,j}). \quad (2)$$

Here, the external ( $V_{ext}$ ) plus screened ( $V_H + \Sigma$ ) terms of Eq. (1) are described by a superposition of atom-centered functions  $v_\alpha$  (where  $\mathbf{d}_{\alpha,j}$  is the position of atom  $j$  of type  $\alpha$  in the  $n$ -th cell  $\mathbf{R}_n$ ). They can be constrained to fit approximately yet accurately the QSGW

calculated SS of bulk solids ( $n = \infty$ ) [25] and of low-period ( $n \sim 2$ ) 2D quantum-wells. In addition, they reproduce well not only the bulk band gaps throughout the Brillouin zone, but also the electron and hole effective-mass tensors, as well as the valence band and conduction band offsets between the well and barrier materials [8, 9, 25]. The spin splitting  $\Delta_i$  of band  $i$  obtained by the direct calculation of Eq. (1) or Eq. (2) will be fitted to the conventional form  $\Delta_i = \alpha_i k + \gamma_i k^3$  for  $i =$  electrons (e) or holes (h), allowing both a linear in  $k$  and a cubic in  $k$  terms to be present.

*Results of the many-body multi-band calculation:* For **3D bulk GaAs**, Fig. 1 compares our multi-band approach to the *ab initio* QSGW for 3D bulk GaAs, showing the linear and cubic SS of the three lowest *conduction bands* (CB1, CB2, and CB3) and three highest *valence bands* (HH, LH, and SO). The coefficients of linear and cubic terms as obtained by fitting the calculated SS to  $\Delta_i(k)$  are given for each band in the inset to Fig. 1. We find that the SS of all bands has a cubic term  $\gamma_i^{(3D)}$ , but only HH, LH, and CB3 with angular momentum  $J = 3/2$  have linear term  $\alpha_i^{(3D)}$ . For these bands the cubic and linear splittings have opposite signs. The screened pseudopotential solution of Eq. (2) gives similar results to QSGW (see inset to Fig. 1). The exception is that Eq. (2) gives  $\alpha_i^{(3D)} = 0$  for all bands because this approach is coreless and this term results from coupling to the core states [10]. Fortunately,  $\alpha_i^{(3D)}$  does not matter much for 2D so we can safely use this method for larger systems.

For **2D (GaAs)<sub>2</sub>/(AlAs)<sub>2</sub> superlattice**, the SS of *electrons* obtained by our atomistic multi-band approach agrees well with **k·p** [21] in that the linear term  $\alpha_e^{(2D)} \propto \alpha_e^{(3D)}/d^2$  originates from the folding-in of 3D bulk cubic term  $\alpha_e^{(3D)}$  due to the confinement to a well of width  $d$ . This is not the case for *holes*. The SS of 2D valence subbands (hh0, lh0, and hh1) is presented in Fig. 2; the first two lines of Table I give the linear and cubic coefficients  $\alpha_{hh0}^{(2D)}$  and  $\gamma_{hh0}^{(2D)}$ . Both atomistic multi-band methods [Eqs. (1) and (2)] show: (i) a linear scaling of SS in addition to a cubic scaling for all three valence subbands including hh0, in contrast to only a cubic scaling of hh0 in the model-Hamiltonian derived by Bulaev and Loss [13]. (ii) The linear term dominates the SS at small  $k$ ;  $\alpha_{hh0}^{(2D)}$ ,  $\alpha_{hh1}^{(2D)}$ , and  $\alpha_{lh0}^{(2D)}$  are comparable.

We next consider a few possible scenarios that might have led to a strong 2D hole splitting, finding all but the last to be unlikely.

(i) *The standard  $2 \times 2$  model Hamiltonian for 2D does not explain the results.* Bulaev and Loss [13] have shown that starting from a  $4 \times 4$  basis in 3D there is no linear terms for hh0 in the 2D model Hamiltonian. However, they did not include the *3D relativistic cubic terms* of  $\Gamma_{8v}$  bands in their derivation. Rashba and Sherman [15] demonstrated earlier that the 3D relativistic cubic terms can give rise to 2D linear term for hh0 subbands [Eq. (8) in Ref. 15]. We tested this idea calculating the 2D SS using a pseudopotential which was constructed to fit the Rashba-Sherman 3D band structure including the relativistic cubic terms. The results of the pseudopotential calculation for 2D (in which all bands are allowed to couple) are compared with the Rashba-Sherman 2D model (in which the 2D hh0 band is uncoupled). Fig. 3 and Table I show that for sufficiently large superlattice periods  $n$ , for which the 2D model of Ref. 15 is applicable, the model recovers only a small fraction of the multi-band results for linear SS of 2D hh0. For smaller periods ( $n \leq 20$ ) we report in Fig. 3 a clear non-monotonic period dependence of both  $\alpha_{hh0}^{(2D)}$  and  $\alpha_{ih0}^{(2D)}$ , with  $\alpha_{hh0}^{(2D)}$  to  $\alpha_{ih0}^{(2D)}$  ratios varying from  $\sim 10$  to  $< 1$  as the period decreases from 50 to 2 ML. This is in sharp contrast with the predictions of the model Hamiltonian [15] which predicts a monotonic increase of linear terms and a ratio of  $\alpha_{hh0}^{(2D)}$  to  $\alpha_{ih0}^{(2D)}$  which is independent of  $d$ .

(ii) *Interfaces induce only minor 2D linear splitting:* In 2D quantum-wells, Foreman [12] suggested an interface induced linear term that originates from valence band coupling to the  $p$ -like  $\Gamma_4$  states. For 2D GaAs/AlAs quantum well, he [12] estimated that independent of period this interfacial linear term is in the range of  $20 - 30$  meVÅ. In contrast, we find for near-bulk (large-period) superlattice such as (GaAs)<sub>80</sub>/(AlAs)<sub>20</sub> (Table I) that  $\alpha_{hh0}^{(2D)}$  is very close to its bulk value of QSGW. Thus, even if we assume that the interfacial linear term is solely responsible for the remaining discrepancy from bulk value, it is even smaller than what was estimated by Foreman [12]. We conclude that the interfacial linear term, if it exists, is only a minor contribution to  $\alpha_{hh0}^{(2D)}$ .

(iii) *Core-valence coupling is not the reason either:* One might have suspected that quantum confinement pushes the valence bands closer to core levels and thus increases the linear term due to increased coupling. This too can be excluded since our screened pseudopotential is a coreless method, yet we find similar results as the all-electron QSGW calculation.

(iv) *Undiscovered spin-orbit linear terms:* The quantitative and qualitative disagreements of atomistic multi-band calculation with the standard model Hamiltonian approach

suggest possible undiscovered SOI terms, which are not included in the model Hamiltonian. Such terms due to symmetry lowering down from 3D  $T_d$  bulk symmetry to 2D  $D_{2d}$  quantum well symmetry could originate from coupling of 3D bands via the 2D potential and SOI. Such coupling is signaled by the distinctly nonparabolic 2D energy dispersion curves manifesting clear anti-crossings between neighboring subbands, multi-band calculation displayed in the inset to Fig. 3. In the model Hamiltonian approach [13, 15] the hh0, hh1, ..., wavefunctions near zone-center in 2D all derive from a *single* bulk state |HH⟩ and similarly, all lh0, lh1 ..., wavefunctions in 2D derive from a *single* bulk state |LH⟩. However, the inset to Fig. 3 shows that the lh0 level lies *between* the hh0 and hh1 levels in 2D for all multi-band calculated GaAs periods. Clearly, the coupling of 3D states and its effects on SS of 2D bands can not be ignored as done in the model Hamiltonian approach for extremely small-k range [13, 15]. A better approach than this “band decoupled” model Hamiltonian [13, 15] approximation allows the 2D state hh0 to derive from a few bulk states. In such a “mixing of decoupled states” approximation,

$$\Psi_{hh0}^{(2D)} = w_{hh0}^{(2D)}(\text{HH})|\text{HH}\rangle + w_{hh0}^{(2D)}(\text{LH})|\text{LH}\rangle + \dots, \quad (3)$$

where  $w_{hh0}^{(2D)}(\lambda)$  is the percent weight of 3D state  $\lambda = \text{HH}, \text{LH}, \dots$  in the 2D state  $\Psi_{hh0}^{(2D)}$ . In the band decoupled model  $w_{hh0}^{(2D)}(\lambda) \equiv 0$  for  $\lambda \neq \text{HH}$ . We have calculated the weights by numerical projection of the 2D pseudopotential wavefunctions and show them in Fig. 4. In striking contrast to the assumption made in model Hamiltonian approach, the interband coupling is large even at zone center. We see that for long-period (GaAs thickness  $\geq 20$  ML)  $\Psi_{hh0}^{(2D)}$  is made of 90% |HH⟩ and 5% |LH⟩, but for shorter periods the mixing *increases*: the HH content drops to  $\sim 70 - 80$  % and the LH content raises to 10 – 20 %. This monotonically enhanced mixing of LH and HH into the 2D hh0 as the QW period is reduced signals the breakdown of the model Hamiltonian thinking that neglects such mixing on the ground that the energy splitting of hh0-lh0 must be larger than that of hh0-hh1 for sufficient small periods [13].

The linear coefficient of 2D hh0 SS can be written in terms of the weights in Eq. (3) in a model of “mixing of decoupled states” as

$$\alpha_{hh0}^{(2D)} = -w_{hh0}^{(2D)}(\text{HH})\tilde{\alpha}_{hh0}^{(2D)} + w_{hh0}^{(2D)}(\text{LH})\tilde{\alpha}_{lh0}^{(2D)} + \dots, \quad (4)$$

where  $\tilde{\alpha}_{hh0}^{(2D)}$  ( $\tilde{\alpha}_{lh0}^{(2D)}$ ) is the contribution of a single bulk HH (or LH) band to linear SS of 2D hh0 subband, which had been derived by Rashba and Sherman [15] (the negative sign

accounts for band repulsion effect). The result of the first two terms in Eq. (4) is shown as open squares in Fig. 3 and are compared with the Multi-band calculated  $\alpha_{hh0}^{(2D)}$  (solid circles). We see that the mixing of decoupled states [Eq. (4)] gives a much better approximation to the full calculation than the model Hamiltonian treating one decoupled band at the time (open circles in Fig.3) [26]. Thus, the mixing of bulk bands leads to a large linear SS of 2D hh0, and is unsuspected by the standard model that judge coupling by energy proximity.

The emergence of a large linear term for Dresselhaus hole SS in 2D nanostructures suggests (i) the dominance of Dresselhaus over Rashba SOI (having a cubic term as its lowest order term) [13], (ii) a larger spin-Hall effect [16], and (iii) an explanation of the observed large optical anisotropy [12]. The occurrence of a larger SS of hh0 corresponding to HH-LH coupling leads to a short hole spin-relaxation time in 2D quantum-wells [6] from the D'Yakonov and Perel (DP) mechanism [7].

A.Z. thanks E. Rashba and D. Loss for helpful discussions on this subject. Work at NREL was funded by the U.S. Department of Energy, Office of Science, Basic Energy Science, Materials Sciences and Engineering, under Contract No. DE-AC36-08GO28308 to NREL. MvS was supported by ONR, project N00014-07-1-0479.

- 
- [1] G. Dresselhaus, Phys. Rev. **100**, 580 (1955).
  - [2] Y.A. Bychkov and E.I. Rashba, J. Phys. C **17**, 6039 (1984).
  - [3] S. Murakami, N. Nagaosa, S.C. Zhang, Science **301**, 1348 (2003).
  - [4] D. Brunner, *et al*, Science **325**, 70 (2009).
  - [5] D. Heiss, S. Schaeck, H. Huebl, M. Bichler, G. Abstreiter, J. J. Finley, D. V. Bulaev, and Daniel Loss, Phys. Rev. B **76**, 241306(R) (2007).
  - [6] I. A. Yugova, A. A. Sokolova, D. R. Yakovlev, A. Greilich, D. Reuter, A. D. Wieck, and M. Bayer, Phys. Rev. Lett. **102**, 167402 (2009)
  - [7] *Optical Orientation*, edited by B.P. Zakharchenya and F. Meier (North-Holland, Amsterdam, 1984).
  - [8] A. Zunger, phys. stat. sol. (a) **190**, 467 (2002).
  - [9] R. Magri and A. Zunger, Phys. Rev. B **64** 081305(R) (2001).
  - [10] M. Cardona, N.E. Christensen, and G. Fasol, Phys. Rev. B **38**, 1806 (1988).

- [11] E. L. Ivchenko, A. Yu. Kaminski, and U. Rössler, Phys. Rev. B **54**5852 (1996).
- [12] B.A. Foreman, Phys. Rev. Lett. **86**, 2641 (2001); and references therein.
- [13] D. V. Bulaev and D. Loss, Phys. Rev. Lett. **95**, 076805 (2005).
- [14] R. Winkler, *Spin-orbit Coupling Effects in Two-Dimensional Electron and Hole Systems*, (Springer, 2003).
- [15] E.I. Rashba and E.Ya. Sherman, Phys. Lett. A **129**, 175 (1988).
- [16] B.A. Bernevig and S.C. Zhang, Phys. Rev. Lett. **95**, 016801 (2005).
- [17] M.F. Borunda, T. S. Nunner, T. Luck, N. A. Sinitsyn, C. Timm, J. Wunderlich, T. Jungwirth, A. H. MacDonald, and J. Sinova, Phys. Rev. Lett. **99**, 066604 (2007)
- [18] D. Stepanenko, M. Lee, G. Burkard, and D. Loss, Phys. Rev. B **79** 235301 (2009)
- [19] O. Olendski, Q. L. Williams, and T. V. Shahbazyan, Phys. Rev. B **77** 125338 (2008)
- [20] J. Schliemann and D. Loss, Phys. Rev. B **71** 085308 (2005)
- [21] R. Eppenga and M.F.H. Schuurmans, Phys. Rev. B **37**, 10923 (R) (1988).
- [22] M. van Schilfgaarde, T. Kotani, and S. Faleev, Phys. Rev. Lett. **96**, 226402 (2006).
- [23] A.N. Chantis, M. van Schilfgaarde, and T. Kotani, Phys. Rev. Lett. **96**, 086405 (2006).
- [24] J.J. Krich and B.I. Halperin, Phys. Rev. Lett., **98**, 226802 (2007).
- [25] J.W. Luo, G. Bester, and A. Zunger, Phys. Rev. Lett. **102** 056405 (2009).
- [26] The discrepancy of Eq. (4) from the multi-band calculation for  $n < 20$  implies that there are additional SOI induced interband coupling for small GaAs period  $n$ , as evidenced by significantly enhanced band mixing (see Fig. 4).



TABLE I: The coefficients of linear and cubic terms  $\alpha_i^{(2D)}$  and  $\gamma_i^{(2D)}$  for 2D superlattice as well as 3D bulk GaAs. Here  $\alpha_i^{(2D)}$  units in meVÅ and  $\gamma_i^{(2D)}$  in eVÅ<sup>3</sup>. The symbol in parentheses denotes the character of the folded-in band (bulk  $\Gamma$ -like or X-like) at the Brillouin-zone center  $\bar{\Gamma}$  of the 2D system. We show results from QSGW [Eq. (1)] as well as from screened pseudopotential [Eq. (2)]. The pseudopotential used for 2D system in this Table was constructed specifically to predict comparable bulk SS to model Hamiltonian result [15] (see text) rather than QSGW values.

Superlattice (GaAs) <sub>n</sub> /(AlAs) <sub>m</sub>	CB1		VB1	
	$\alpha_e^{(2D)}$	$\gamma_e^{(2D)}$	$\alpha_{hh0}^{(2D)}$	$\gamma_{hh0}^{(2D)}$
<i>GW</i> : 2/2 ( <i>X</i> )	61.5	0.2	102.6	151.3
PP: 2/2 ( <i>X</i> )	37.8	22.1	339.6	15.4
PP: 2/4 ( <i>X</i> )	8.5	0.2	352.9	1.5
PP: 2/10 ( <i>X</i> )	23.0	2.2	379.1	13.2
PP: 2/20 ( <i>X</i> )	20.0	10.5	420.2	13.2
PP: 20/20 ( $\Gamma$ )	71.7	12.2	206.1	95.9
PP: 30/20 ( $\Gamma$ )	41.5	7.3	114.5	111.8
PP: 50/20 ( $\Gamma$ )	17.9	3.6	50.4	126.6
PP: 80/20 ( $\Gamma$ )	7.7	1.5	22.1	113.6
PP: 3D GaAs	0.0	<b>21.6</b>	0.0	<b>8.3</b>
<i>GW</i> : 3D GaAs	0.0	<b>8.5</b>	12.6	<b>3.1</b>

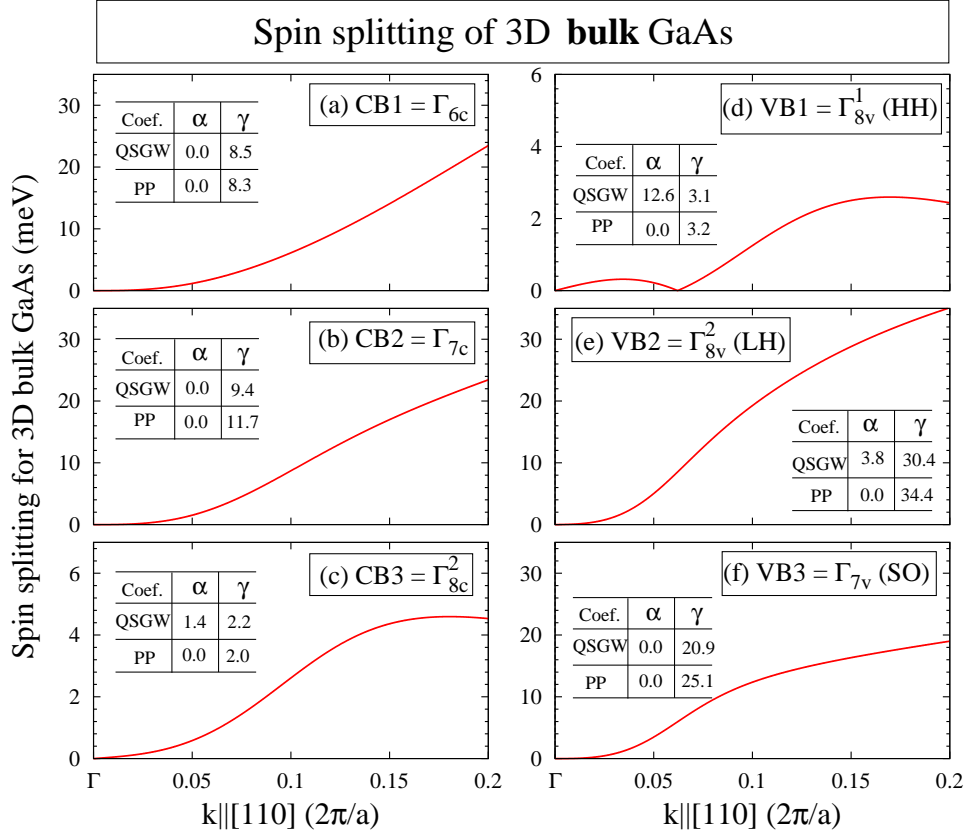


FIG. 1: (color online) QSGW predicted SS of 3D bulk GaAs for the three lowest conduction bands (a) CB1, (b) CB2, and (c) CB3, and three highest valence bands (d) VB1, (e) VB2, and (f) VB3. Dresselhaus constants  $\alpha_i$  in  $\text{meV}\text{\AA}$  and  $\gamma_i$  in  $\text{eV}\text{\AA}^3$  predicted by QSGW and screened pseudopotential fit to QSGW, respectively, are given for each band in the inset.

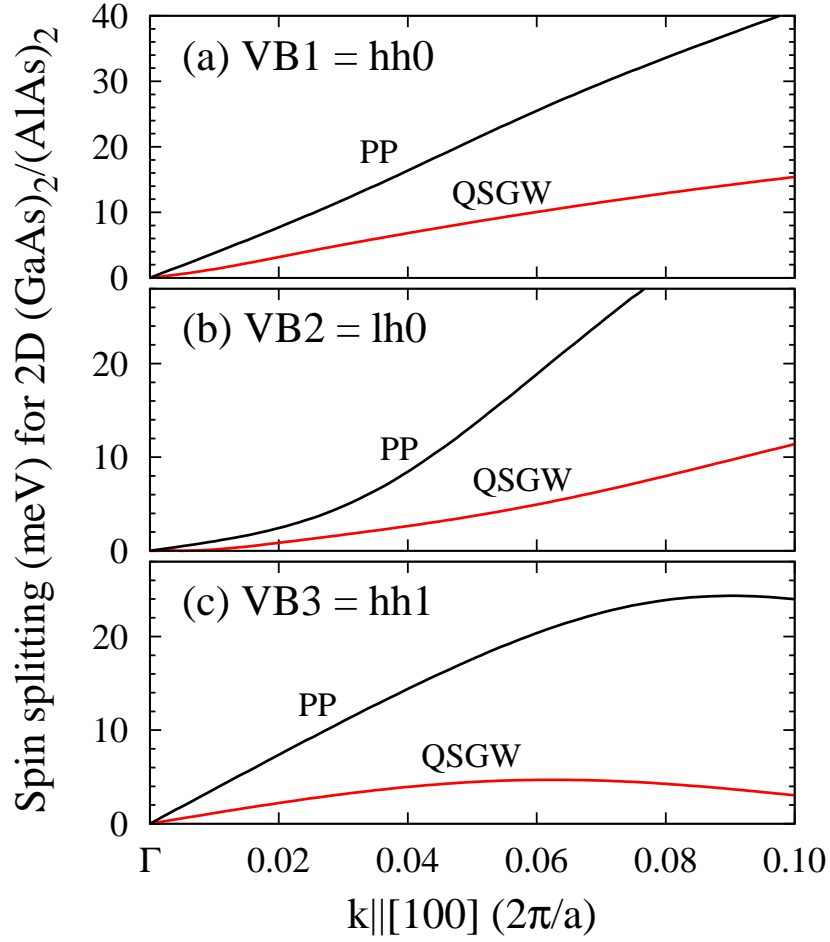


FIG. 2: QSGW [Eq. (1)] predicted SS (red line) of 2D  $(\text{GaAs})_2/(\text{AlAs})_2$  superlattice for the three highest valence subbands (a) hh0, (b) lh0, and (c) hh1. The corresponding SS calculated by screened pseudopotential fit to model Hamiltonian result [15] [Eq. (2)] is also given in black line for each subband.

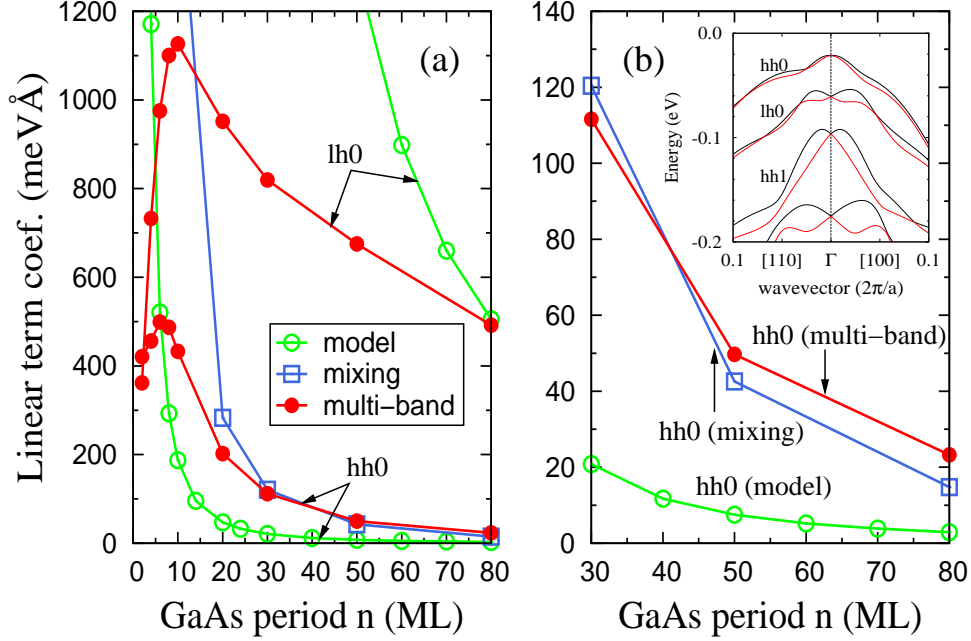


FIG. 3: (a) Comparison of linear SS coefficients  $\alpha_{hh0}^{(2D)}$  and  $\alpha_{lh0}^{(2D)}$  calculated from present pseudopotential multi-band approach (same as in Table I; solid circles), as well as by the Rashba-Sherman model Hamiltonian (open circles), and mixing approximation [Eq. (4); open squares] for 2D  $(\text{GaAs})_n/(\text{AlAs})_{20}$  quantum wells. (b) Expanded scale for long-period QW's highlighting the comparison of hh0 subbands for the direct calculation *vs* model Hamiltonian and mixing approximation. Inset shows energy dispersion of valence subbands for 2D  $(\text{GaAs})_n/(\text{AlAs})_{20}$  calculated by atomistic pseudopotential approach. The two spin subbands for each orbit subband are represented by low energy red line and a high energy black line.

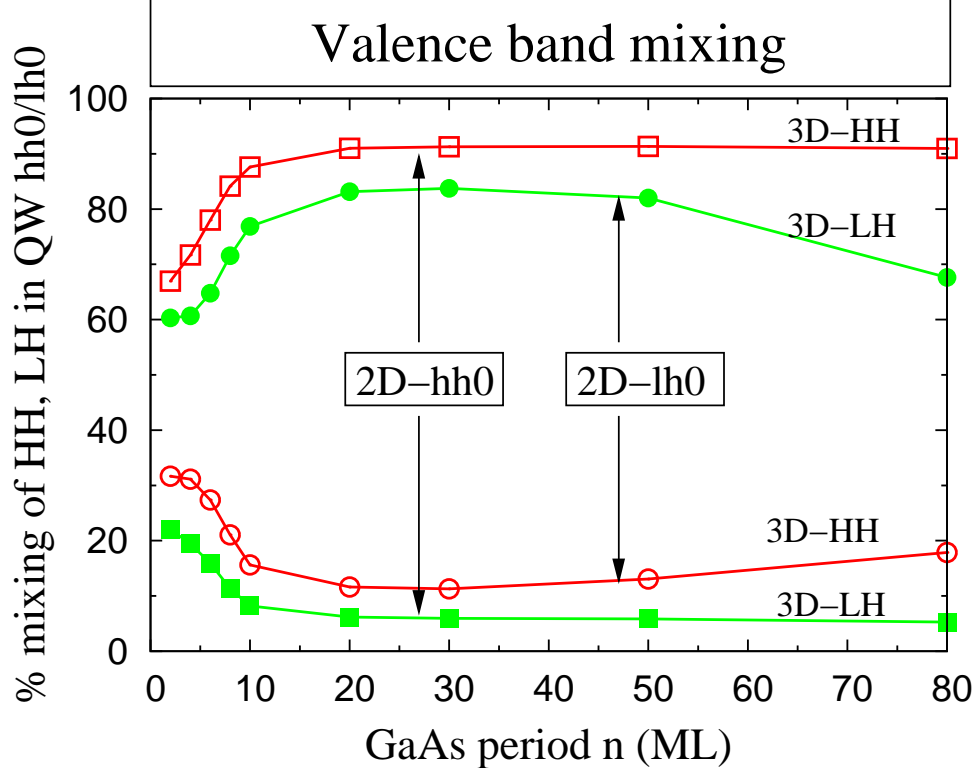


FIG. 4: Percent of bulk HH and LH bands mixed into the 2D hh0 and lh0 subbands at zone center calculated by numerical projection. The results are almost same in a small in-plane  $k$  range [e.g.,  $k < 0.01(2\pi/a)$ ]. Note that the sum of bulk HH and LH content is less than 100%. In our atomistic multi-band calculation, the subband ordering from top to bottom is hh0, lh0, hh1, ... for all GaAs period.